

Defects in pathfinding by cranial neural crest cells in mice lacking the neuregulin receptor ErbB4

Jon P. Golding*†, Paul Trainor†‡, Robb Krumlauf‡ and Martin Gassmann*§

*Division of Neurobiology, National Institute for Medical Research, The Ridgeway, Mill Hill, London NW7 1AA, UK

‡Division of Developmental Neurobiology, National Institute for Medical Research, The Ridgeway, Mill Hill, London NW7 1AA, UK

§e-mail: mgassma@nimr.mrc.ac.uk

†These authors contributed equally to this work

Mouse embryos with a loss-of-function mutation in the gene encoding the receptor tyrosine kinase ErbB4 exhibit misprojections of cranial sensory ganglion afferent axons. Here we analyse ErbB4-deficient mice, and find that morphological differences between wild-type and mutant cranial ganglia correlate with aberrant migration of a subpopulation of hindbrain-derived cranial neural crest cells within the paraxial mesenchyme environment. In transplantation experiments using new grafting techniques in cultured mouse embryos, we determine that this phenotype is non-cell-autonomous: wild-type and mutant neural crest cells both migrate in a pattern consistent with the host environment, deviating from their normal pathway only when transplanted into mutant embryos. ErbB4 signalling events within the hindbrain therefore provide patterning information to cranial paraxial mesenchyme that is essential for the proper migration of neural crest cells.

During vertebrate development, cranial neural crest cells (NCCs) migrate along highly stereotyped routes within the mesenchyme and contribute to the forming bone, cartilage and peripheral nervous system of the developing head. From the outset, NCC migration pathways are segmented, mirroring the underlying segmentation of the hindbrain neuroepithelium into lineage-restricted compartments called rhombomeres¹. Thus, NCCs from rhombomeres (r)2, r4 and r6 migrate laterally through the cranial mesenchyme in three distinct, sharply defined streams that do not enter the intervening mesenchyme adjacent to r3 or r5 (refs 2–5). Similarly, at slightly later ages, primary sensory afferent axons of the trigeminal and geniculate/cochleovestibular ganglia grow through cranial mesenchyme and into the hindbrain through distinct entry sites in r2 and r4, respectively.

The results of previous studies have indicated that the mesenchyme adjacent to r3 and r5 may contain an activity that excludes NCCs^{6,7}. So far, relatively few molecules that influence the pathfinding of craniofacial NCCs have been identified, but examples include ephrins and their receptors, Eph proteins^{8,9}, and evidence is emerging to indicate that collapsin-1/semaphorin-III might also be involved¹⁰. Ephrins and semaphorin-III also can affect the pathfinding of axons^{11,12}, including cranial ganglion axons in the case of semaphorin III¹². Hence it appears that molecules influencing NCC migration may also be used for axon guidance.

Another molecule required for pathfinding by cranial ganglion axons is the receptor tyrosine kinase ErbB4 (ref. 13), which has cognate ligands that include the neuregulins^{14–17}, betacellulin¹⁸ and heparin-binding epidermal growth factor^{15,19}. In the developing mouse hindbrain, ErbB4 is expressed within r3 and r5 from embryonic day (E) 8. By E9, expression shifts to the margins of r3 and r5, where it becomes concentrated throughout the dorsoventral extent of the pial surface at the rhombomere boundaries^{20,21}. Unlike in the developing central nervous system, ErbB4 expression has not been detected during the period of cranial neurogenesis in migrating NCCs, developing cranial ganglia, or paraxial mesenchyme in either mice or chicks^{20,22}.

In mice with a loss-of-function mutation in the *ErbB4* gene, a subset of centrally projecting trigeminal and geniculate/cochleovestibular ganglia afferent axons become misdirected and grow through r3-adjacent mesenchyme towards each other's entry sites²⁰. Further-

more, the trigeminal ganglion and the geniculate/cochleovestibular ganglia complex of *ErbB4* mutant embryos at E10 are displaced towards each other²⁰, perhaps as a consequence of the aberrant axon projections between them, but also raising the alternative possibility that cranial ganglion precursor cells, which derive from the neural crest and ectodermal placodes²³, may show abnormalities in pathfinding or migration. Hence, ErbB4, like ephrins and semaphorin-III, may have a role in the pathfinding of both axons and NCCs. Here we analyse ErbB4-deficient mice further, and find that ErbB4 signalling events within the hindbrain are indeed essential for the correct migration of a subpopulation of NCCs.

Results

Anatomical changes in cranial ganglia of ErbB4-deficient embryos. To assess abnormalities in the cranial ganglia of ErbB4-deficient (*ErbB4*^{-/-}) embryos at E10, we performed whole-mount *in situ* hybridization analysis using the neuronal marker NeuroD²⁴. This analysis revealed highly reproducible differences in the distribution of neurons between *ErbB4* mutants and control littermates. The trigeminal (gV) and geniculate/cochleovestibular (gVII/gVIII) ganglia were closer together in all mutant embryos ($n > 30$) than in wild-type littermates, although these ganglia always remained discrete and were never fused into a single ganglion (Fig. 1). In mutant embryos there was a caudal extension of the trigeminal ganglion into the dorsal mesenchyme adjacent to r3 (Fig. 1a–f). The geniculate ganglion (gVII) was also modestly elongated, a feature that was more clearly observed using a Phox2b probe (Fig. 2e–h). In some cases (~25%), an ectopic geniculate ganglion was present more ventrally, near the geniculate epibranchial placode (Fig. 1d, h, small arrow). In contrast, the size and position of the cochleovestibular ganglion (gVIII) was the same in both wild-type and mutant embryos.

NeuroD is transiently expressed by all terminally differentiating cranial ganglion neurons²⁴. Therefore, to help us to resolve the origins of sensory neurons populating the abnormal regions of mutant ganglia, we used three more markers, namely Neurogenin-1, which labels neurons derived from neural crest, otic placode and trigeminal placode²⁵; Neurogenin-2, which labels neurons within the epibranchial placodes²⁶; and Phox2b, which labels placodal-derived

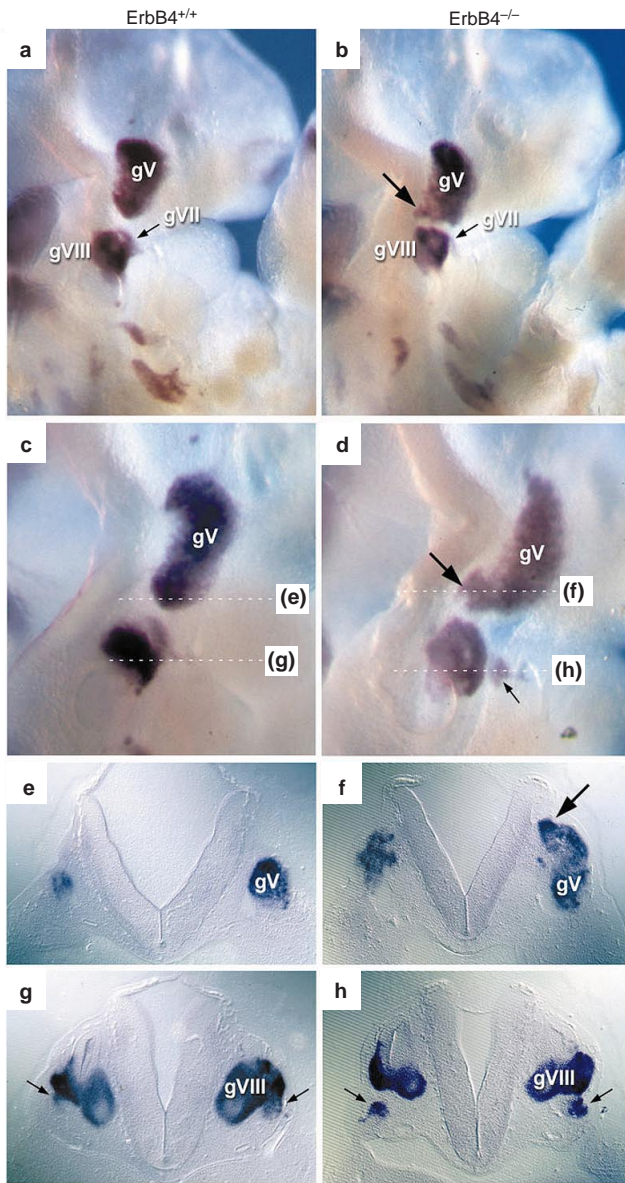


Figure 1 Cranial ganglion abnormalities in *ErbB4*^{-/-} embryos. Wild-type (**a, c, e, g**) and *ErbB4*^{-/-} (**b, d, f, h**) mouse embryos at E10 were processed for whole-mount *in situ* hybridization with the pan-neuronal marker *NeuroD*. **a, b**, Side views; **c, d**, more dorsal views of the cranial region at higher magnification; **e–h**, transverse sections. **b** and **d** show two different *ErbB4*^{-/-} embryos, to illustrate the range of the phenotype. In *ErbB4*^{-/-} embryos, the *NeuroD* probe revealed a caudal extension of the trigeminal (gV) ganglion (large arrows in **b, d**; shown in transverse section in **f**; large arrow). The geniculate (gVII) ganglion was also elongated, mostly caudally (small arrow in **b**), and in some cases an ectopic gVII was formed just ventral to the cochleovestibular (gVIII) ganglion complex (small arrow in **d**); the ectopic gVII is more easily seen in transverse section (gVII is indicated by small arrows in **g, h**). Dotted lines in **c, d** show the planes of the sections taken for **e–h**.

cells within the geniculate, petrosal and nodose ganglia²⁷. In E10 mutant embryos, *Neurogenin-1* revealed a similar caudal extension in the trigeminal ganglion (gV) to that seen with *NeuroD* (compare Fig. 2a, b with Fig. 1). The geniculate ganglion was not stained, as it derives from the facial epibranchial placode²³ (Fig. 2a, b). *Neurogenin-2* showed a slightly more disorganized and diffuse staining pattern at E8.5 in the mutant geniculate epibranchial placode

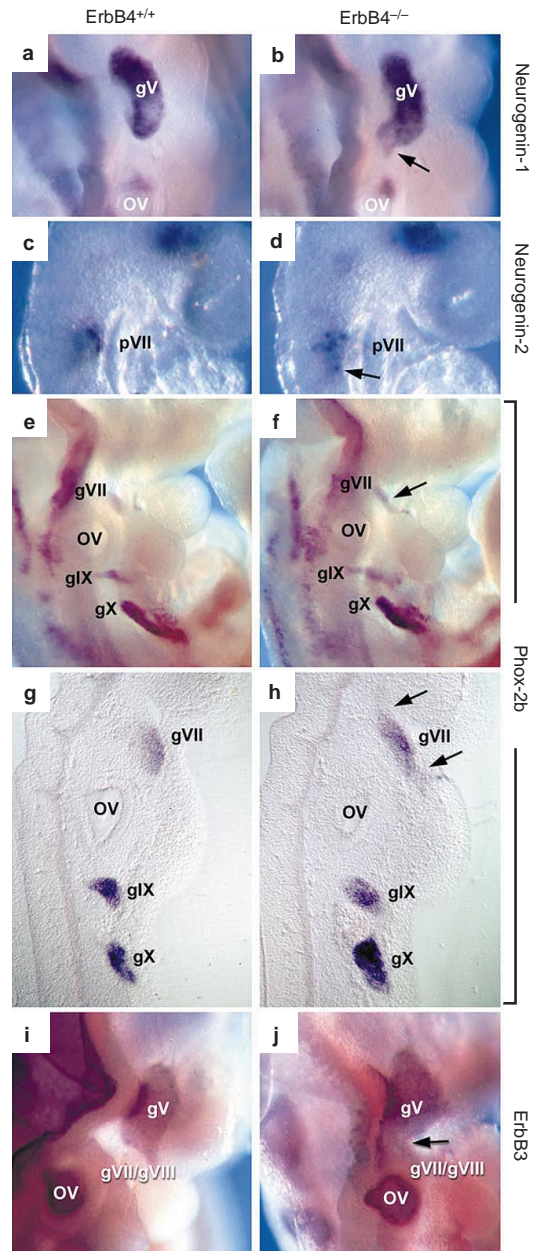


Figure 2 Neural crest cells and placode-derived cells contribute to the *ErbB4*^{-/-} phenotype. Wild-type (**a, c, e, g, i**) and *ErbB4*^{-/-} (**b, d, f, h, j**) embryos were processed for whole-mount *in situ* hybridization with probes that identify NCCs and/or placodal-derived cells. **a, b**, The *Neurogenin-1* probe revealed a caudal extension of the trigeminal ganglion (gV) in E10 *ErbB4*^{-/-} embryos (arrow in **b**); this extension could consist of either neural crest or placodal cells. **c, d**, The *Neurogenin-2* probe revealed a more diffuse geniculate epibranchial placode (pVII) in E8.5 *ErbB4*^{-/-} embryos (arrow in **d**). **e–h**, Similarly, in E10 *ErbB4*^{-/-} embryos, the *Phox2b* probe revealed an elongation of the placode-derived geniculate ganglion (gVII) (arrow in **f**), more clearly seen in longitudinal section (**g, h**; arrows in **h**). **i, j**, The *ErbB3* probe, which identifies developing neural sheath cells, was expressed in gV and the gVII/gVIII complex of E10 wild-type embryos (**i**). In *ErbB4*^{-/-} E10 embryos (**j**), a band of *ErbB3*-expressing cells was present between gV and gVII/gVIII (arrow). In all cases, rostral is towards the top. OV, otic vesicle; gIX, petrosal ganglion; gX, nodose ganglion.

(pVII) (Fig. 2c, d), and *Phox2b* revealed both a rostral and a caudal elongation of the geniculate ganglion (gVII) in mutants compared with wild-type embryos at E10 (Fig. 2e–h).

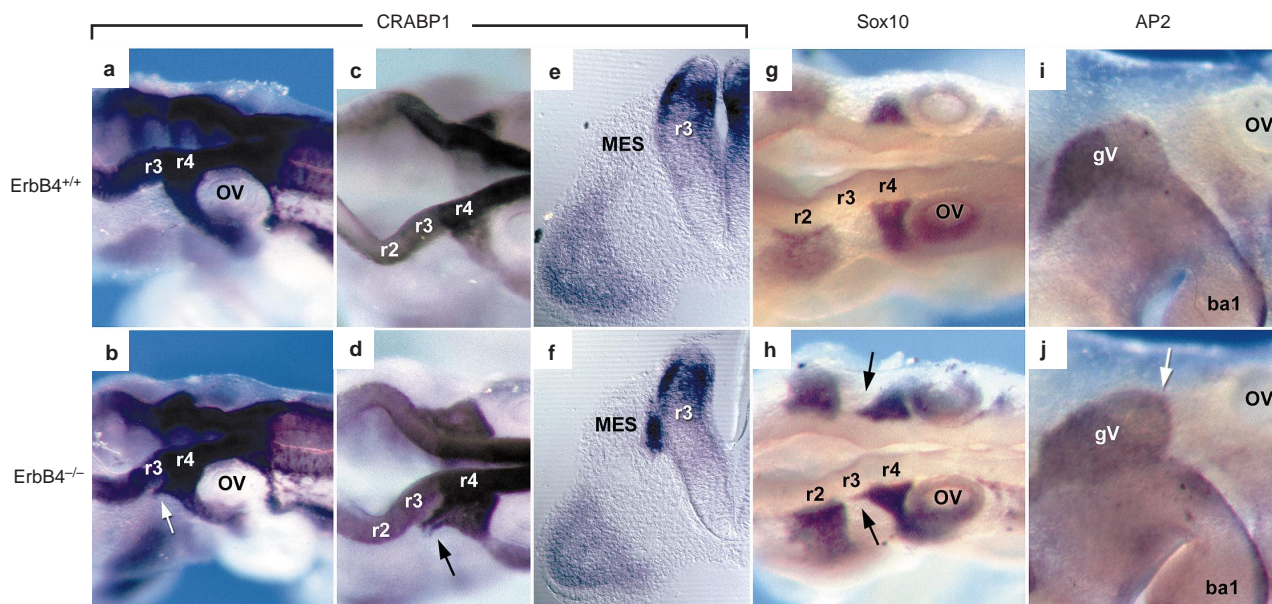


Figure 3 A subpopulation of r4-derived neural crest cells is misguided in *ErbB4*^{-/-} embryos. **a–h**, Whole-mount *in situ* hybridizations using the NCC markers CRABP1 (**a–f**) and Sox10 (**g, h**) on E9 wild-type (**a, c, e, g**) and E9 *ErbB4*^{-/-} (**b, d, f, h**) embryos reveal that a subpopulation of r4-derived NCCs becomes deviated rostrally through r3-adjacent mesenchyme in *ErbB4*^{-/-} embryos (arrows in **b, d, h**). In

transverse section (**e, f**) at the level of r3, the aberrant CRABP1-expressing crest can be seen in *ErbB4*^{-/-} embryos (**f**) within the mesenchyme (MES) lying adjacent to the neuroepithelial basal lamina. **i, j**, *In situ* hybridization at E10 using the NCC marker AP2 reveals the caudal extension of the trigeminal ganglion (gV) in *ErbB4*^{-/-} embryos (arrow in **j**). OV, otic vesicle; ba1, branchial arch 1.

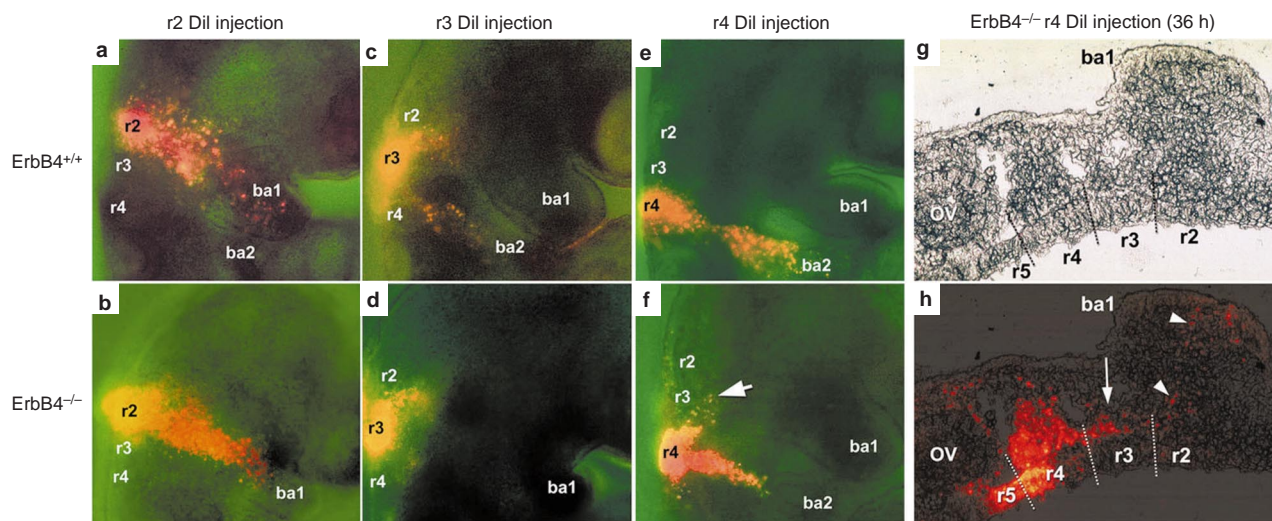


Figure 4 Dil labelling confirms that the migration of only r4-derived neural crest cells is affected in *ErbB4*^{-/-} embryos. **a–f**, NCCs in individual rhombomeres of wild-type (**a, c, e**) and *ErbB4*^{-/-} (**b, d, f**) E8 embryos were labelled with Dil and then cultured for 24 h. No differences were seen in the migration patterns of r2 (**a, b**) or r3 (**c, d**) NCCs from wild-type or *ErbB4*^{-/-} embryos (note that only in cases where r3 was overfilled with Dil, possibly labelling some of r2 and r4, were cells seen to migrate out into the adjacent r2 or r4 crest streams). Only when NCCs in r4 were labelled with Dil (**e, f**) could differences be seen in the patterns of migration of wild-type and *ErbB4*^{-/-} NCCs. In *ErbB4*^{-/-} embryos, r4-derived NCCs migrated

aberrantly into r3-adjacent mesenchyme (arrow in **f**). **g, h**, When *ErbB4*^{-/-} embryos injected with Dil in r4 were allowed to develop for a longer period, for 36 h, labelled NCCs were still detected in r3-adjacent mesenchyme (arrow in **h**); some labelled cells were also detected in r2-adjacent mesenchyme and in the first branchial arch (arrowheads in **h**). **a–f**, Whole-mount embryos; **g, h** show the same longitudinal section of a *ErbB4*^{-/-} embryo, where **g** shows a bright-field image and **h** shows a superimposition of bright-field and Dil-fluorescence images. OV, otic vesicle; ba1, branchial arch 1; ba2, branchial arch 2.

In addition to these sensory neurons, we also studied glia by examining the distribution of NCC-derived nerve sheath cells using an *ErbB3* probe²⁸ (Fig. 2i, j). In wild-type embryos, *ErbB3* labelled

cells in discrete ganglia (Fig. 2i). However, in mutant embryos expression appeared in a continuous group of cells extending from the trigeminal ganglion (gV) to the geniculate/cochleovestibular

ganglia complex (gVII/gVIII) (Fig. 2j, arrow). This expression pattern is consistent with the idea that sheath cells are associated with the subpopulation of axons that misproject between the trigeminal and geniculate/cochleovestibular ganglia in mutant embryos²⁰. Taken together, these data indicate that the cranial ganglia abnormalities in *ErbB4* mutants may result from altered migration (or premature differentiation) of placodal cells in the case of the geniculate ganglion, and from altered migration of NCCs and/or placodal cells in the case of the trigeminal ganglion.

A subpopulation of r4 NCCs migrate aberrantly in *ErbB4*^{-/-} embryos. To determine whether NCC derivatives are involved in establishing the mutant phenotype of the trigeminal ganglion, we looked for variations in the pathways taken by migrating NCCs, using CRABP1 as a marker²⁹ (Fig. 3a–f). In mutant embryos, CRABP1 revealed an aberrant stream of NCCs that branched off the r4-derived neural crest stream at the dorsoventral level of the otic vesicle. These NCCs projected rostrally through the mesenchyme adjacent to r3 (Fig. 3b, d) in close association with the neuroepithelial basal lamina (Fig. 3f). CRABP1 is weakly expressed by r2 NCCs and we therefore used another NCC marker, Sox10 (ref. 30), to determine whether there were also any abnormalities in the patterning of the r2-derived neural crest stream. As with CRABP1, the Sox10 probe revealed an aberrant, rostrally migrating population of r4 NCCs within r3-adjacent mesenchyme (Fig. 3h). However, we detected no differences in Sox10-expressing r2 NCCs (compare Fig. 3g, h). Analysis with another NCC marker, AP2 (ref. 31), showed the caudal extension of the trigeminal ganglion in *ErbB4* mutants at later stages of development (E10) (Fig. 3j). The results of our analyses of NCC markers support the idea that r4-derived neurogenic NCC derivatives contribute to the caudal extension of the trigeminal ganglion in *ErbB4*^{-/-} embryos.

DiI tracing reveals the presence of misrouted NCCs originating from r4. To determine directly whether the misrouted NCCs in mutant embryos did indeed derive from r4, we DiI-labelled premigratory NCCs in r2, r3 or r4 at E8. After culturing the embryos for 24 h we studied the migratory pathways that these cells had taken (Fig. 4). We found no differences between the pathways taken by r2-derived (Fig. 4a, b) or r3-derived (Fig. 4c, d) NCCs in wild-type or mutant embryos. In both wild-type (*n* = 20) and mutant (*n* = 6) embryos, relatively few NCCs were seen to migrate from r3; those that did migrated rostrally and caudally to join NCCs in adjacent r2 and r4, as described previously⁴. In no cases were r3-derived NCCs observed to migrate laterally into the adjacent r3 mesenchyme.

In wild-type embryos (*n* = 20), r4-derived NCCs migrated laterally and ventrally as a single stream into the second branchial arch (Fig. 4e). In contrast, in mutant embryos (*n* = 18 out of 20), a subpopulation of DiI-labelled r4-derived NCCs migrated rostrally through the dorsal cranial mesenchyme adjacent to r3 and r2 (compare Fig. 4e, f). In about half of the mutant embryos, some labelled r4-derived NCCs also deviated caudally towards the otic vesicle (Fig. 4f). In other embryos (*n* = 5), we deliberately injected r4 with DiI caudally, away from the r3/r4 boundary, to ensure that r4-derived, and not r3-derived, NCCs were labelled. After culturing these embryos for 36 h (to E9.5), we could see clearly that, in mutant embryos, r4-derived NCCs had migrated rostrally through the mesenchyme adjacent to r3 and r2, and that small numbers of these cells had joined the stream of r2-derived NCCs and migrated into the first branchial arch (Fig. 4g, h). Hence, in contrast to wild-type embryos, in *ErbB4* mutants r4-derived NCCs contribute to derivatives of both the first and the second branchial arches.

Misdirected r4-derived NCCs are a late-migrating subpopulation. r4-derived NCCs that migrated correctly into the second branchial arch had always migrated further than the ectopic or misdirected r4 NCCs (Fig. 4e, f). To study the dynamics of the mutant NCC phenotype, we bred the *ErbB4* mutation into a *Hoxb2/lacZ* transgenic background (ML22 line^{32,33}) that specifically expressed the reporter gene in r4 and in r4-derived NCCs. *Hoxb2/lacZ* *ErbB4*^{-/-} and *Hoxb2/lacZ* *ErbB4*^{+/-} embryos were collected at ages ranging from

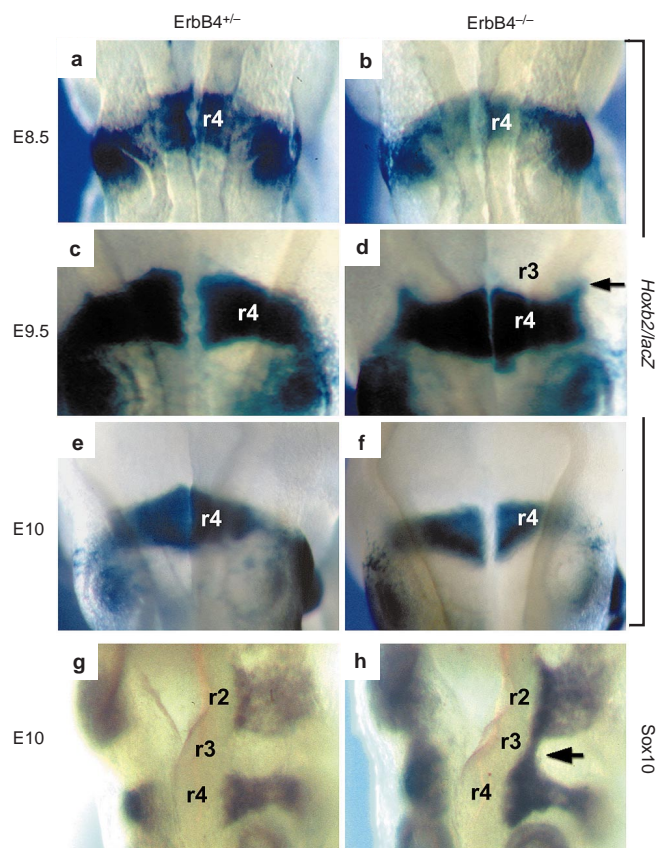


Figure 5 Misguided r4-derived neural crest cells are a late-migrating subpopulation. a–f, Dorsal views of X-gal-stained *ErbB4*^{+/-} (a, c, e) and *ErbB4*^{-/-} (b, d, f) embryos expressing *Hoxb2/lacZ* reporters, which specifically label r4 and migrating r4-derived NCCs. Misguided r4-derived NCCs in *Hoxb2/lacZ* *ErbB4*^{-/-} embryos are not seen at the earliest age studied (E8.5), but are observed later, at E9.5 (arrow in d). At E10, however, misguided cells can no longer be seen in *Hoxb2/lacZ* *ErbB4*^{-/-} embryos (compare d, f), even though cells within the r4 neural crest stream maintain *lacZ* expression at E10 (f). g, h, Whole-mount *in situ* hybridizations with Sox10 in age-matched E10 *ErbB4*^{+/-} (g) and *ErbB4*^{-/-} (h) embryos show the continued presence of misguided neural crest cells within r3-adjacent mesenchyme of mutant embryos (arrow in h). Rostral is towards the top.

E8.5 to E10. At E8.5, X-gal staining showed no aberrant migration of *Hoxb2/lacZ*-expressing r4 NCCs in *ErbB4* mutants, even though r4-derived NCCs had migrated normally into the second branchial arch by this age (Fig. 5a, b). In contrast, by E9.5 a subpopulation of r4-derived NCCs had migrated aberrantly adjacent to r3 (Fig. 5c, d). These results indicate that the *ErbB4* mutation may mainly affect late-migrating neural crest cells.

Interestingly, by E10, reporter expression in mutants appeared to be lost specifically in those cells that migrated ectopically in an anterior direction, as opposed to those that migrated laterally (Fig. 5e, f). The downregulation of reporter expression in the misdirected stream adjacent to r3 could reflect a change in cell fate or the elimination of the ectopic population, for example by cell death. To investigate these possibilities, we studied the expression of the NCC marker Sox10 in age-matched E10 embryos. In contrast to wild-type embryos (Fig. 5g), mutant embryos showed strong Sox10 expression in an NCC stream adjacent to r3 (Fig. 5h), indicating that misdirected NCCs were still present in the ectopic positions at E10 in *ErbB4*^{-/-} embryos. These results indicate that some aspects of NCC identity may be specified by local environmental cues within the cranial mesenchyme, as the expression of *Hoxb2* is not maintained by r4-derived NCCs that migrate into the ectopic r3-adjacent

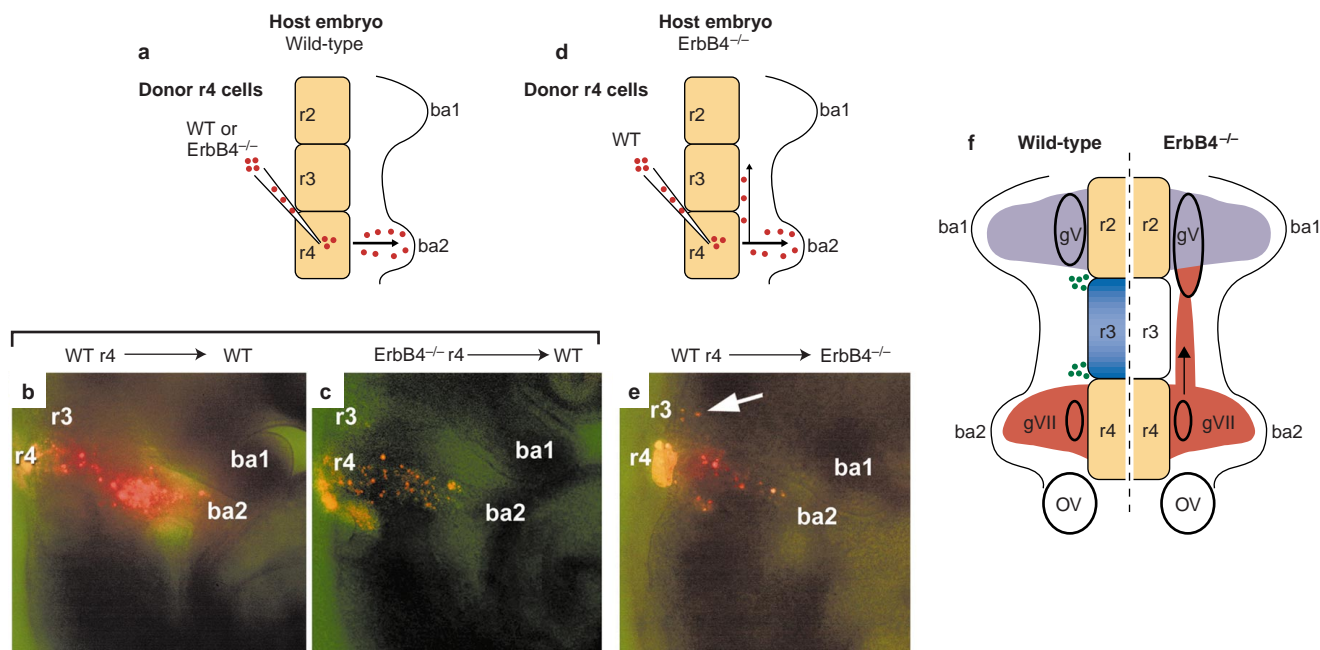


Figure 6 Environmental, not crest-intrinsic, cues control the misrouting of neural crest cells in *ErbB4*^{-/-} embryos. **a–e**, Transplantation paradigms are summarized in **a** and **d**, while the corresponding whole-mount fluorescence photographs of cultured embryos are shown in **b**, **c** and in **e**, respectively. **a–c**, Wild-type (WT; **b**) or *ErbB4* mutant (**c**) r4 cells were grafted into the premigratory r4 neural crest territory of wild-type host embryos (as shown in **a**) and the subsequent migration of the DiI-labelled cells was monitored after 24 h of embryo culture. Both wild-type and mutant cells migrated normally in the wild-type hosts. **d, e**, Wild-type r4 cells were grafted into the premigratory r4 neural crest territory of *ErbB4* mutant host embryos as shown in **d**, and their subsequent migration was assessed after 24 h in culture (**e**). The arrow in **e** denotes the aberrant migration of wild-type cells in the mutant host environment. **f**, Summary of the results shown in **b**, **c**, **e**, and model of the neural crest phenotype in *ErbB4* mutant embryos. In wild-type embryos (left),

ErbB4 is expressed within r3 neuroepithelium (blue), while an *ErbB4* ligand, neuregulin-1, is expressed in the adjacent r2 and r4 (yellow). Thus, *ErbB4*-mediated cell signalling is probably focused at the r3/r2 and r3/r4 boundaries (indicated by the darker blue shading within r3), where it stimulates the secretion of putative NCC-migration inhibitors/repellents (green dots) that accumulate in the adjacent r3 mesenchyme. Thus, neural crest streams from r2 (purple) and r4 (red) remain segregated. In *ErbB4*^{-/-} embryos (right), *ErbB4* signalling is disrupted in r3 (lack of blue shading) and the inhibitory/repellent activity is not produced. A subpopulation of r4-derived NCCs migrates aberrantly through r3-adjacent mesenchyme (arrow) and contributes to an ectopic caudal extension of the trigeminal ganglion (gV). ba1, branchial arch 1; ba2, branchial arch 2; gV, trigeminal ganglion; gVII, geniculate ganglion; OV, otic vesicle.

mesenchyme position, even though *Hoxb2* continues to be expressed by appropriately located r4-derived NCCs in the second arch. The idea that changes in environmental cues along the anteroposterior axis of the cranial mesenchyme can influence NCC identity is supported by the results of recent NCC-transplantation experiments in mouse embryos³⁴.

Migration pathway of r4 NCCs is determined by local environmental cues. It was unclear whether the misguiding of certain r4-derived NCCs in *ErbB4*^{-/-} embryos resulted from altered patterning cues within the mesenchyme environment or from changes intrinsic to the NCCs. To resolve this problem, we adopted a chimaeric approach, taking advantage of a new and powerful cell-grafting technique^{33,34} in combination with lineage tracing and embryo culture. First we tested whether the aberrant migration of r4-derived NCCs was intrinsic to the mutant cells. We grafted wild-type or *ErbB4* mutant r4 cells into the premigratory r4 neural crest territory of wild-type host embryos (Fig. 6a), and studied the subsequent migration of the DiI-labelled cells. When either wild-type or *ErbB4* mutant r4 cells were transplanted into wild-type host embryos, the graft-derived NCCs migrated normally as a single stream within the host mesenchyme and populated the second branchial arch (Fig. 6b, c). These results show that the mutant cells possess the ability to respond to a normal environment.

Next, to determine whether the environment is altered in *ErbB4* mutant embryos, we grafted wild-type r4 cells into the premigratory r4 neural crest territory of *ErbB4* mutant host embryos (Fig. 6d), and studied their subsequent migration. In contrast to the previous situation, a subpopulation of wild-type r4 cells in the mutant back-

ground migrated aberrantly into the mesenchyme adjacent to r3 (Fig. 6e, arrow). Hence, these transplanted wild-type cells must no longer be receiving the proper signals to direct their appropriate migration. Together these results indicate that the *ErbB4* mutation is not NCC-autonomous, but instead affects guidance cues within the mesenchymal environment through which r4 NCCs migrate. As *ErbB4* is expressed in the neuroepithelium, but not in the mesenchymal environment^{20,35,36}, its effects on guidance cues must involve signalling between the hindbrain and its adjacent mesenchymal tissue.

Discussion

We have shown previously that in mouse embryos with a loss-of-function *ErbB4* mutation, the trigeminal ganglion and geniculate/cochleovestibular ganglia are displaced towards each other, and that cranial ganglion axons from these ganglia misproject towards each other through the intervening r3-adjacent mesenchyme²⁰. We have now provided evidence that the abnormal caudal extension of the trigeminal ganglion of *ErbB4*^{-/-} embryos correlates with the aberrant migration of a subpopulation of r4-derived NCCs into dorsolateral r3-adjacent mesenchyme. Furthermore, we have shown that this phenotype is non-cell-autonomous and that aberrant migration is accompanied by an apparent downregulation of *Hox* gene expression. These results underscore the importance of environmental signals in guiding NCC migration and in regulating NCC identity.

Several previously described mutations or experimental manipulations that affect the pathfinding of neural-crest-derived cells in the developing vertebrate head involve respecification of rhom-

bomere segment identity. This may occur by, for instance, misexpression or overexpression of *Hox* genes^{37,38}, or by exposure to retinoic acid^{39,40}. However, neither changes in *Hoxb2* (Fig. 5) and *Hoxb1* (ref. 20) expression nor any morphological changes²⁰ have been observed within the hindbrain of *ErbB4* mutant embryos that might suggest rhombomere respecification. This raises important questions with respect to how segmental identity and NCC patterning are coordinated.

So far, relatively few molecules have been identified that influence NCC migration in the developing vertebrate head. Those molecules that have been identified include members of the ephrin and Eph families of guidance molecules^{8,9,11} and possibly collapsin-1/semaphorin-III^{10,12}. Ephrins and their Eph receptors are expressed in complementary patterns by the neural crest and/or mesoderm of the *Xenopus* second and third branchial arches, respectively^{8,9}. When either ephrin-B2 (ref. 9) or kinase-deficient EphA2 (ref. 8) is overexpressed in the *Xenopus* hindbrain, migrating NCCs are no longer constrained to their discrete pathways and intermingle within the branchial arches. Furthermore, ephrin-B2 can inhibit NCC migration *in vitro*⁴¹. Although we cannot exclude the possibility that ephrins/Eph receptors may be involved in the *ErbB4* mutant phenotype, the observation that, in *ErbB4* mutant embryos, abnormal NCC migration is confined predominantly to the dorsal mesenchyme, in proximity to the neuroepithelium, argues against this idea. Another candidate for controlling NCC migration is collapsin-1/semaphorin III. During the period of NCC migration, collapsin-1 is regionally expressed within the avian hindbrain, initially in r3 and r5 (ref. 42). In addition, migrating NCCs express the collapsin-1 receptor, neuropilin-1, and avoid patterned stripes of collapsin-1 *in vitro*¹⁰.

All of the molecules described above that regulate the migration pattern of cranial NCCs also influence axon pathfinding in various systems. In the case of *ErbB4* and semaphorin III, cranial ganglion axon misprojections have been described in the respective knockout mice^{12,20}. Furthermore, members of the collapsin/semaphorin gene family, as well as the Eph receptors and their ephrin ligands, are well established as molecules that regulate axon guidance in several areas of the developing nervous system^{43,44}. Taken together, these findings support the theory that similar molecular and cellular mechanisms are used for neural crest and axon pathfinding, within the developing vertebrate head, and it will be important to determine how these mechanisms and pathways are integrated to control normal development.

In Fig. 6f, we propose a model in which *ErbB4* has a role in NCC migration, and show the phenotypic consequences arising from the absence of *ErbB4*. As the cranial mesenchyme does not express *ErbB4* either before or during the period of NCC migration^{20,21,35,36}, it is unlikely to be the direct source of the *ErbB4*-dependent NCC-patterning information we describe here. Instead, *ErbB4*-expressing neuroepithelial cells in r3 are ideally placed to provide patterning cues that restrict migrating NCCs from entering r3-adjacent mesenchyme. These patterning cues could be either inhibitory molecules secreted directly from the neuroepithelium, or molecules induced secondarily within the mesenchyme under the control of neuroepithelial-derived signals. At least one ligand for *ErbB4*, neuropilin-1, is expressed in r2 and r4, where it could activate *ErbB4* signalling pathways in r3 (ref. 28). Experiments in chick embryos are consistent with the idea that a diffusible inhibitory activity is released from r3. Thus, grafting experiments in which quail r2 or r4 tissue is transplanted into host chick mesenchyme reveal that donor NCCs fail to migrate into mesenchyme adjacent to r3 or r5 (ref. 7). In other experiments, when r3/r4-adjacent mesenchyme is surgically rotated before NCC migration, r4-derived NCCs can migrate laterally into the ectopically placed r3 mesenchyme⁴⁵, indicating that the putative r3-derived inhibitory activity may need to be continually replenished within the mesenchyme adjacent to r3.

We have recently provided evidence that there is a neurite-growth inhibitor in the r3-adjacent mesenchyme that patterns cen-

tral projections of cranial sensory axons and that this inhibitor might be absent in *ErbB4*^{-/-} embryos²¹. It is tempting to speculate that this axon-growth-inhibitory activity is the same as that which we propose restricts NCC migration into r3-adjacent mesenchyme. However, as the pathfinding of r2-derived NCCs is unaffected in *ErbB4*^{-/-} embryos, it must be assumed that further, *ErbB4*-independent signalling pathways operate.

In summary, our data emphasize the importance of hindbrain-to-mesenchyme signals in regulating the appropriate pathways for migrating NCCs and growing axons in the developing vertebrate head. Future work will be directed at identifying the *ErbB4*-dependent factor(s) that patterns cranial NCC migration, and whether this factor(s) acts independently or cooperatively with other patterning cues. □

Methods

Animals and embryo isolation for cultures.

Embryos were obtained from timed-pregnant matings of heterozygous *ErbB4* mutants²⁰, and from crosses of *ErbB4* mutants with a transgenic line in which reporter expression is driven by an r4-specific enhancer from *Hoxb2* (construct ML22; ref. 32). The *ErbB4* mutant genotype of embryos was confirmed by polymerase chain reaction (PCR) analysis of yolk-sac genomic DNA using *ErbB4*-specific primers²⁰.

Embryos for use in culture experiments were dissected from the uterus with an intact visceral yolk sac, amnion and ectoplacental cone⁴⁶. Host embryos at E8.5 were cultured *in vitro* for 24 h in DR50 medium in a 5% O₂, 5% CO₂, 90% N₂ atmosphere and, if required, they were cultured for a further 12 h in DR75 in a 20% O₂, 5% CO₂, 75% N₂ atmosphere⁴⁷. To catch the earliest waves of migrating neural crest cells in lineage-tracing and rhombomere-grafting experiments, we used only donor and host embryos having six or fewer pairs of somites.

In situ hybridization.

The following mouse complementary DNA templates were used: *NeuroD*, *Neurogenin-1*, *Neurogenin-2*, *Phox2b*, *Sox10*, *CRABP1*, *AP2* and *ErbB3*. Antisense digoxigenin-labelled riboprobes were synthesized from linearized templates by the incorporation of digoxigenin-labelled UTP (Boehringer), using either T3 or T7 RNA polymerase. Whole-mount *in situ* hybridizations were performed with 400 ng ml⁻¹ riboprobe according to ref. 48, using alkaline-phosphatase-conjugated anti-digoxigenin antibody and NBT-BCIP substrate (Boehringer).

NCC lineage-tracing experiments.

In both *ErbB4*^{-/-} and wild-type embryos at E8.5, we focally injected the dorsal region of individual rhombomeres with a small quantity of Dil (0.05% w/v; Molecular Probes) as described^{29,50}. These dye-injected embryos were cultured *in vitro* for up to 36 h. Numbers of injections were as follows: wild-type controls, n > 20 each for r2, r3 and r4; *ErbB4* mutants, r2: n = 10, r3: n = 6, r4: n = 20.

Isolation of rhombomeres.

Consistent neuromeric landmarks were used to identify the rhombomeric source of tissue to be grafted and the correct site of transplantation⁴⁹. Finely polished alloy and glass needles were used to separate the neuroectoderm from adjacent tissues. Rhombomeres that could not be cleanly separated from adjacent tissues were then incubated in 0.5% trypsin, 0.25% pancreatin, 0.2% glucose and 0.1% polyvinylpyrrolidone in PBS for 3 min at 37 °C or in 0.1% dispase for 3 min at 37 °C to ensure a pure population. Isolated rhombomeres were then washed in DMEM before being labelled with a 1:1 mix of Dil:DR50 for 2 min. The labelled tissue was again washed in DMEM before being dissected with glass needles into smaller fragments consisting of ~10–15 cells, suitable for transplantation into the dorsal region of the neural tube⁵¹.

Rhombomere-transplantation experiments.

Small groups of ~15 cells isolated from r4 of E8.5 embryos were reciprocally transplanted homotopically between wild-type CBA and *ErbB4*^{-/-} embryos. These embryos were cultured for 24 h *in vitro*. Numbers of grafts were as follows: wild-type r4 into wild-type hosts, n = 20; *ErbB4* mutant r4 into wild-type hosts, n = 14; wild-type r4 into *ErbB4* mutant hosts, n = 12.

RECEIVED 7 DECEMBER 1999; REVISED 29 DECEMBER 1999; ACCEPTED 5 JANUARY 2000; PUBLISHED 14 JANUARY 2000.

- Lumsden, A. & Krumlauf, R. Patterning the vertebrate neuraxis. *Science* **274**, 1109–1115 (1996).
- Noden, D. M. An analysis of migratory behavior of avian cephalic neural crest cells. *Dev. Biol.* **42**, 106–130 (1975).
- Lumsden, A., Sprawson, N. & Graham, A. Segmental origin and migration of neural crest cells in the hindbrain region of the chick embryo. *Development* **113**, 1281–1291 (1991).
- Sechrist, J., Serbedzija, G. N., Scherson, T., Fraser, S. E. & Bronner-Fraser, M. Segmental migration of the hindbrain neural crest does not arise from its segmental generation. *Development* **118**, 691–703 (1993).
- Birgbauer, E., Sechrist, J., Bronner-Fraser, M. & Fraser, S. Rhombomeric origin and rostrocaudal reassortment of neural crest cells revealed by intravitral microscopy. *Development* **121**, 935–945 (1995).
- Keynes, R. J., Jaques, K. F. & Cook, G. M. Axon repulsion during peripheral nerve segmentation. *Development Suppl* **2**, 131–139 (1991).
- Farlie, P. G. *et al.* A paraxial exclusion zone creates patterned cranial neural crest cell outgrowth adjacent to rhombomeres 3 and 5. *Dev. Biol.* **213**, 70–84 (1999).
- Helbling, P. M., Tran, C. T. & Brandli, A. W. Requirement for EphA receptor signaling in the segregation of *Xenopus* third and fourth arch neural crest cells. *Mech. Dev.* **78**, 63–79 (1998).

9. Smith, A., Robinson, V., Patel, K. & Wilkinson, D. G. The EphA4 and EphB1 receptor tyrosine kinases and ephrin-B2 ligand regulate targeted migration of branchial neural crest cells. *Curr. Biol.* **7**, 561–570 (1997).
10. Eickholt, B. J., Mackenzie, S. L., Graham, A., Walsh, F. S. & Doherty, P. Evidence for collapsin-1 functioning in the control of neural crest migration in both trunk and hindbrain regions. *Development* **126**, 2181–2189 (1999).
11. Holder, N. & Klein, R. Eph receptors and ephrins: effectors of morphogenesis. *Development* **126**, 2033–2044 (1999).
12. Ulupinar, E., Datwani, A., Behar, O., Fujisawa, H. & Erzurumlu, R. Role of semaphorin III in the developing rodent trigeminal system. *Mol. Cell. Neurosci.* **13**, 281–292 (1999).
13. Plowman, G. D. *et al.* Ligand-specific activation of HER4/p180erbB4, a fourth member of the epidermal growth factor receptor family. *Proc. Natl Acad. Sci. USA* **90**, 1746–1750 (1993).
14. Plowman, G. D. *et al.* Heregulin induces tyrosine phosphorylation of HER4/p180erbB4. *Nature* **366**, 473–475 (1993).
15. Riese, D. J. *et al.* The epidermal growth factor receptor couples transforming growth factor- α , heparin-binding epidermal growth factor-like factor, and amphiregulin to Neu, ErbB-3, and ErbB-4. *J. Biol. Chem.* **271**, 20047–20052 (1996).
16. Zhang, D. *et al.* Neuregulin-3 (NRG3): a novel neural tissue-enriched protein that binds and activates ErbB4. *Proc. Natl Acad. Sci. USA* **94**, 9562–9567 (1997).
17. Harari, D. *et al.* Neuregulin-4: a novel growth factor that acts through the ErbB-4 receptor tyrosine kinase. *Oncogene* **18**, 2681–2689 (1999).
18. Beerli, R. R. & Hynes, N. E. Epidermal growth factor-related peptides activate distinct subsets of ErbB receptors and differ in their biological activities. *J. Biol. Chem.* **271**, 6071–6076 (1996).
19. Paria, B. C., Elenius, K., Klagsbrun, M. & Dey, S. K. Heparin-binding EGF-like growth factor interacts with mouse blastocysts independently of ErbB1: a possible role for heparan sulfate proteoglycans and ErbB4 in blastocyst implantation. *Development* **126**, 1997–2005 (1999).
20. Gassmann, M. *et al.* Aberrant neural and cardiac development in mice lacking the ErbB4 neuregulin receptor. *Nature* **378**, 390–394 (1995).
21. Golding, J. P., Tidcombe, H., Tsoni, S. & Gassmann, M. Chondroitin sulphate-binding molecules may pattern central projections of sensory axons within the cranial mesenchyme of the developing mouse. *Dev. Biol.* **216**, 85–97 (1999).
22. Dixon, M. & Lumsden, A. Distribution of neuregulin-1 (nrg1) and erbB4 transcripts in embryonic chick hindbrain. *Mol. Cell. Neurosci.* **13**, 237–258 (1999).
23. D'Amico-Martel, A. & Noden, D. Contributions of placodal and neural crest cells to avian cranial peripheral ganglia. *Am. J. Anat.* **166**, 445–468 (1983).
24. Lee, J. E. *et al.* Conversion of *Xenopus* ectoderm into neurons by NeuroD, a basic helix-loop-helix protein. *Science* **268**, 836–844 (1995).
25. Ma, Q., Chen, Z., del Barco Barrantes, I., de la Pompa, J. L. & Anderson, D. J. neurogenin1 is essential for the determination of neuronal precursors for proximal cranial sensory ganglia. *Neuron* **20**, 469–482 (1998).
26. Fode, C. *et al.* The bHLH protein NEUROGENIN 2 is a determination factor for epibranchial placode-derived sensory neurons. *Neuron* **20**, 483–494 (1998).
27. Pattyn, A., Morin, X., Cremer, H., Goridis, C. & Brunet, J.-F. Expression and interactions of the two closely related homeobox genes *Phox2a* and *Phox2b* during neurogenesis. *Development* **124**, 4065–4075 (1997).
28. Meyer, D. *et al.* Isoform-specific expression and function of neuregulin. *Development* **124**, 3575–3586 (1997).
29. Ruberte, E., Friederich, V., Morriss-Kay, G. & Chambon, P. Differential distribution patterns of CRABP-I and CRABP-II transcripts during mouse embryogenesis. *Development* **115**, 973–989 (1992).
30. Kuhlbrodt, K., Herbarth, B., Sock, E., Hermans-Borgmeyer, I. & Wegner, M. Sox10, a novel transcriptional modulator in glial cells. *J. Neurosci.* **18**, 237–250 (1998).
31. Mitchell, P. J., Timmons, P. M., Hébert, J. M., Rigby, P. W. J. & Tjian, R. Transcription factor *AP-2* is expressed in neural crest cell lineages during mouse embryogenesis. *Genes Dev.* **5**, 105–119 (1991).
32. Maconochie, M. *et al.* Cross-regulation in the mouse HoxB complex: the expression of *Hoxb2* in rhombomere 4 is regulated by *Hoxb1*. *Genes Dev.* **11**, 1885–1896 (1997).
33. Manzanares, M. *et al.* The role of kreisler in segmentation during hindbrain development. *Dev. Biol.* **211**, 220–237 (1999).
34. Trainor, P. & Krumlauf, R. Plasticity in mouse neural crest cells reveals a new patterning role for cranial mesoderm. *Nature Cell Biol.* **2**, 96–102 (2000).
35. Meyer, D. & Birchmeier, C. Multiple essential functions of neuregulin in development. *Nature* **378**, 386–390 (1995).
36. Gassmann, M. & Lemke, G. Neuregulins and neuregulin receptors in neural development. *Curr. Opin. Neurobiol.* **7**, 87–92 (1997).
37. Alexandre, D. *et al.* Ectopic expression of *Hoxa-1* in the zebrafish alters the fate of the mandibular arch neural crest and phenocopies a retinoic acid-induced phenotype. *Development* **122**, 735–746 (1996).
38. Bell, E., Wingate, R. J. & Lumsden, A. Homeotic transformation of rhombomere identity after localized *Hoxb1* misexpression. *Science* **284**, 2168–2171 (1999).
39. Lee, Y. M. *et al.* Retinoic acid stage-dependently alters the migration pattern and identity of hindbrain neural crest cells. *Development* **121**, 825–837 (1995).
40. Gale, E. *et al.* Late effects of retinoic acid on neural crest and aspects of rhombomere. *Development* **122**, 783–793 (1996).
41. Wang, H. U. & Anderson, D. J. Eph family transmembrane ligands can mediate repulsive guidance of trunk neural crest migration and motor axon outgrowth. *Neuron* **18**, 383–396 (1997).
42. Shepherd, I., Luo, Y., Raper, J. A. & Chang, S. The distribution of collapsin-1 mRNA in the developing chick nervous system. *Dev. Biol.* **173**, 185–199 (1996).
43. Tessier-Lavigne, M. & Goodman, C. S. The molecular biology of axon guidance. *Science* **274**, 1123–1133 (1996).
44. O'Leary, D. D. & Wilkinson, D. G. Eph receptors and ephrins in neural development. *Curr. Opin. Neurobiol.* **9**, 65–73 (1999).
45. Sechrist, J., Scherson, T. & Bronner-Fraser, M. Rhombomere rotation reveals that multiple mechanisms contribute to segmental pattern of hindbrain neural crest migration. *Development* **120**, 1777–1790 (1994).
46. Trainor, P. A., Tan, S. S. & Tam, P. P. L. Cranial paraxial mesoderm-regionalization of cell fate and impact on craniofacial development in mouse embryos. *Development* **120**, 2925–2932 (1994).
47. Sturm, K. & Tam, P. P. L. Isolation and culture of whole postimplantation embryos and germ layer derivatives. *Methods Enzymol.* **225**, 164–190 (1993).
48. Wilkinson, D. G. & Nieto, M. A. Detection of messenger RNA by in situ hybridization to tissue sections and whole mounts. *Methods Enzymol.* **225**, 361–373 (1993).
49. Trainor, P. A. & Tam, P. P. L. Cranial paraxial mesoderm and neural crest of the mouse embryonic distribution in the craniofacial mesenchyme but distinct segregation in the branchial arches. *Development* **121**, 2569–2582 (1995).
50. Quinlan, G. A., Trainor, P. A. & Tam, P. P. Cell grafting and labeling in postimplantation mouse embryos. *Methods Mol. Biol.* **97**, 41–59 (1999).

ACKNOWLEDGEMENTS

We thank S. Tsoni for technical assistance; M. Dixon and B. Fritzsche for critically reviewing the manuscript; H. Tidcombe for valuable discussions; D.J. Anderson and Q. Ma for the gift of *NeuroD*, *Neurogenin-1* and *Neurogenin-2* plasmids; C. Goridis for the *Phox2b* plasmid; and M. Wegner for the *Sox10* plasmid. P.T. was supported by EMBO and HFSP postdoctoral fellowships. This work was funded by Core MRC Programme support and an EEC Biotechnology Network grant (BIO4 CT-960378) to R.K. Correspondence and requests for materials should be addressed to M.G.